CDF/ANAL/EXOTIC/CDFR/6414
June 1, 2003
Version 4.0

Limit Calculation and Incorporation of Systematic Effects in a Search for $WH \to \ell\nu b\bar{b}$

Christopher Neu, Richard Hughes, Phillip Koehn, Evelyn Thomson, Brian Winer
The Ohio State University

Abstract

This note describes the procedure used to calculate limits in a Run 1 search for $WH \to \ell\nu b\bar{b}$. The calculation is described first considering the expected signal and background contributions without regard to the effect of systematic errors. Limits on the WH production cross section are calculated for a spectrum of observation scenarios, as well as the ensemble *a priori* limit. The impact of various sources of systematic error are outlined, followed by a description of how these uncertainties affect the limit calculation. For M_H= 120 GeV, the *a priori* limit on WH production including systematic effects is determined to be 10.0 pb, an increase of 19% over the limit calculated without these uncertainties. The 95% CL *a priori* limit on $\sigma(WH)$ was determined for the range 100 < M_H < 150 GeV.

1 Changes in Version 4.0

The primary change in v4.0 of this document are the rectification of typographical errors on the effect of the tag rate uncertainty in Tables 6, 7 and Tables 11-16 in the Appendix. The changes were merely cosmetic; the correct tag efficiency uncertainty was used in the counting experiments in the determination of limits.

2 Changes in Version 3.0

Changes in v3.0 include:

- use of background and signal event expectations that incorporate tagging scale factor

- employeemt of the current $t\bar{t}$ cross section: 6.5 ± 1.7 pb

The Run1 data results of this analysis are documented in [11].

3 Changes in Version 2.0

Several minor changes were incorporated in v2.0 of this document:

- Extension of the analysis to other masses in the range $100 < M_H < 150$ GeV. While the same NN was used in advanced selection for each M_H value, the $M_{j_1 j_2}$ cut was re-optimized at each M_H. The systematic effects were studied at for M_H= 110,120, and 140; these values were then fitted to approximate the systematic effects for M_H= 100,135,150.
- A 25% uncertainty on the Class 4 and 5 backgrounds has been incorporated per the recommendation from pre-blessing. The value 25% was chosen because it is in the range of the cumulative uncertainty on the Class 2 and class 3 backgrounds, both $\sim 30\%$. Formerly this uncertainty had been assumed to be zero, which clearly was not right.
- The correct Run 1 luminosity 105.1 ± 4 pb^{-1} has now been employed.

4 Introduction

We are performing a Run 1 search for WH production in the $\ell\nu b\bar{b}$ final state. We have utilized a baseline event selection [1] and an advanced selection [2] that are sensitive to the $\ell\nu b\bar{b}$ final state. The selection employed attempts to balance the need for high signal efficiency with the need for large background rejection. Table 1 contains the expected number of signal and background events (split into 4 classes, the motivation for which is described in [2]) considering a Higgs mass of 120 GeV. It is the goal of this note to describe how one translates the event expectations in Table 1 into an a limit measurement.

	Class 1	Class 2	Class 3	Class 4	Class 5
Type of Events	WH	$t\bar{t}$	$W{+}b\,\bar{b}$,$W{+}c\,\bar{c}$,$W{+}c$, W+mistags, non-W	Single top (W-*gluon* and $W*$)	WZ,WW,ZZ, $Z{+}b\,\bar{b}$, $Z{+}c\,\bar{c}$, $Z \rightarrow \tau\tau$
Luminosity	105.1	105.1	105.1	105.1	105.1
Cross Section(pb)	0.14	6.5		1.7, 0.73	
Basic Efficiency	1.2E-2	8.0E-3			
Basic N_{exp}	0.19	5.4	22.7	2.5	2.7
Advanced Efficiency	0.781	0.249	0.319	0.355	0.439
Final N_{exp}	0.15	1.3	7.2	0.9	1.2

Table 1: Run 1 event expectations for signal (M_H= 120 GeV) and the four background classes. Blank entries correspond to values that were not measured in this analysis: the baseline rates of W+QCD-type backgrounds, the diboson channels and the $Z{+}X$ backgrounds were taken from previous Run 1 analyses and were only adjusted by the advanced selection cuts described in [2].

5 Calculating a Limit

From Table 1 we see that $N_{exp}^{S,theory}$= 0.15 and N_{exp}^{B}= 10.6 events. Given these numbers, we seek to calculate the *a priori* 95% confidence level(CL) limit on WH production for the mass hypothesis M_H= 120 GeV.

We first assume that the number of observed events, N_{Obs}, is Poisson distributed:

$$P(x,\mu) = \frac{\mu^x e^{-x}}{x!} \tag{1}$$

where x=N_{Obs}, and μ=the expected number of observed events.

A feature of the Poisson distribution is that its mean and variance are equal; in the above equation, the mean and variance are denoted by μ. Recall that the variance is equal to the width of a distribution squared. The equivalence of mean and variance in the Poisson probability implies that as the mean increases, the impact of the statistical uncertainty (width of Poisson distribution) becomes less critical with respect to the mean value. For example, if we considered a Poisson with mean μ=9 events, then its statistical uncertainty, σ_{stat}, would be 3 events, and the resolution from statistics (σ_{stat}/μ) would be 9/3=0.33, a 33% uncertainty. If instead we consider a Poisson with a mean μ=100, then it would have statistical uncertainty σ_{stat}=10 and resolution of σ/μ = 0.10, a 10% uncertainty. Depending on the mean of the Poisson, the statistical uncertainty for a specific scenario may be significantly greater or significantly smaller than the systematic uncertainty. This is a feature to keep in mind at all times.

In this analysis, the mean of the Poisson is equal to the sum of the number of signal and background events our selection studies predict. Figure 1 shows what this Poisson distribution looks like in N_{Obs} for $\mu = N_{exp}^{S,theory} + N_{exp}^{B}$=10.75 events.

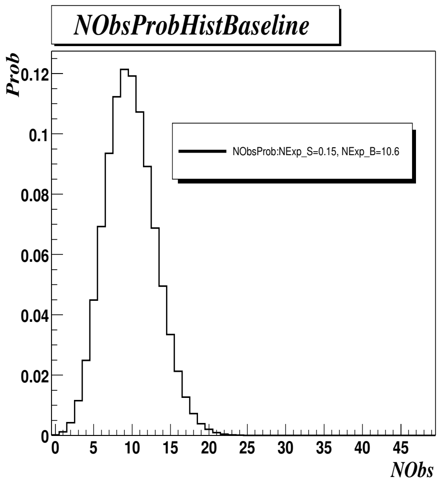

Figure 1: The Poisson distribution in N_{Obs} , with mean and variance equal to $N_{exp}^{S,theory} + N_{exp}^{B}$=10.75 events.$\sigma_{WH}^{theory}$=0.14 pb.

In this analysis, we seek to measure a limit on the WH cross section, so let us ignore for the time being the theory predictions and consider other possible WH cross section values. Figure 2 shows the Poisson distribution in N_{Obs} for σ_{WH}=5,12,20 pb (note that σ_{WH}^{theory}= 0.14 pb).

By constructing these Poissons for various values of σ_{WH}, one can map the entire σ_{WH} versus N_{Obs} plane, pictured in Figure 3. The three curves in Figure 2 represent the three horizontal bins at σ_{WH}=5,12,20 pb in Figure 3. One can see that for $\sigma_{WH}=\sigma_{WH}^{theory}$=0.14 pb, the largest probability scenario predicts N_{Obs}=9 – 12 events, which is a direct result of our expectation $N_{exp}^{S,theory} + N_{exp}^{B}$=10.75 events.

The possible outcomes of this analysis applied to the Run 1 experiment are the different N_{Obs} scenarios plotted along the horizontal axis of Figure 3. Consider a single bin of N_{Obs}, say N_{Obs}=8 events. We can look at the probability distribution for σ_{WH} in this bin, which is pictured in Figure 4. Since

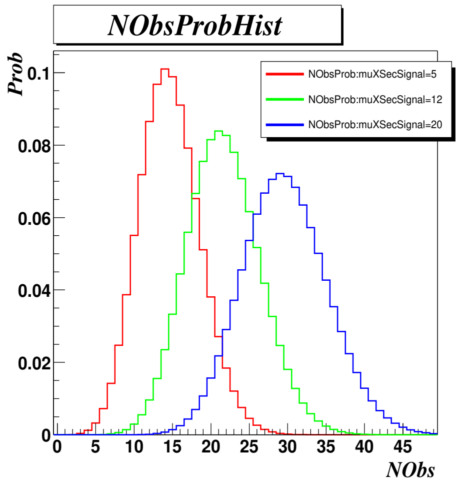

Figure 2: Poissons for σ_{WH}=5,12,20 pb.

we expect $N_{exp}^{S,theory}$+N_{exp}^{B}=10.75 events with σ_{WH}^{theory}=0.14 pb, and since N_{Obs}=8 events corresponds to a deficit with respect to expectation, we see that in the N_{Obs}=8 events bin, small values of σ_{WH} are favored. If we would look at a bin of N_{Obs} that corresponds to an excess over expectation, larger σ_{WH} would be favored.

We refer to the σ_{WH} probability distribution pictured in Figure 4 as the *likelihood* distribution, $\mathcal{L}(\sigma_{WH}|N_{Obs} = 8)$, for σ_{WH} given N_{Obs}= 8 events. In any single N_{Obs} bin, the 95% CL limit on the WH cross section is defined as:

$$0.95 = \frac{\int_0^{\sigma_{WH}^{95}} d\sigma_{WH} \mathcal{L}(\sigma_{WH}|N_{Obs})}{\int_0^{\infty} d\sigma_{WH} \mathcal{L}(\sigma_{WH}|N_{Obs})} \tag{2}$$

Equation 2 just determines the value of σ_{WH} at which 95% of the integrated likelihood distribution is to the left in Figure 4. Figure 5 is the fractional integral plot of the distribution in Figure 4; from Figure 5 we see that for N_{Obs}= 8 events, the 95% CL limit on σ_{WH} is $\approx$ 6.0pb. The 95% CL limit on σ_{WH} can be calculated for each N_{Obs} value; Table 2 contains these limits for several values of N_{Obs}. Recall that σ_{WH}^{theory}= 0.14 pb, for which the total number of expected signal and background was $N_{exp}^{S,theory}$+N_{exp}^{B}=10.75 events.

We seek now the *a priori* limit from this analysis on σ_{WH}. The *a priori* limit incorporates information from all the possible outcomes of the experiment in determining a global limit, weighting the limits from

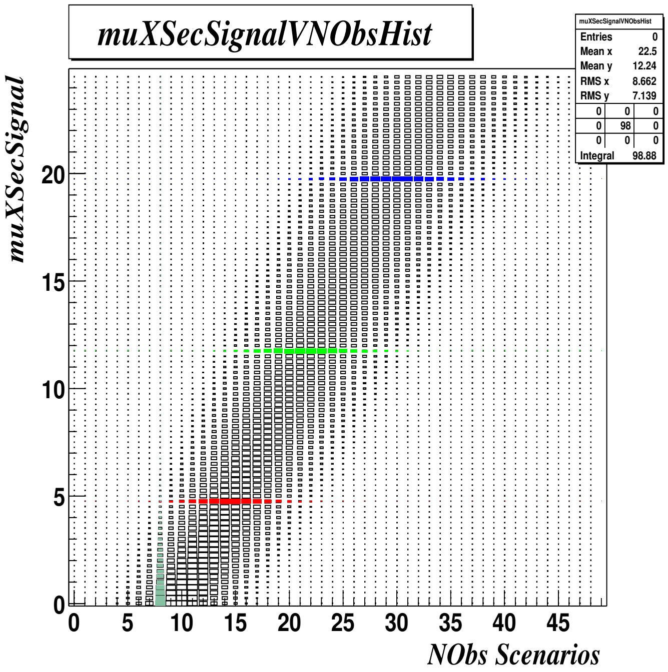

Figure 3: Poisson probabilities of hypothetical σ_{WH} values as a function of N_{Obs}.

each N_{Obs} scenario by their Poisson probability given σ_{WH}=σ_{WH}^{theory}=0.14 *pb*. Thus the *a priori* limit is given by:

$$\sigma_{WH}^{95,apriori} = \sum_{N_{obs}} \sigma_{WH}^{95} * P(N_{obs}|N_{exp}^{S,theory} + N_{exp}^{B}) \tag{3}$$

where $P(x|\mu)$ is the Poisson in x with mean μ. With this prescription,

$$\sigma_{WH}^{95,apriori} = 8.4pb \qquad \text{(no systematics) for } M_H = 120\ GeV$$

Figure 6 contains a summary plot of the 95% CL limits on σ_{WH} for a variety of N_{Obs} scenarios, overlayed with the baseline Poisson for the case in which σ_{WH}=σ_{WH}^{theory}=0.14 *pb*. From Figure 6 one can see that the most probable outcome of our experiment is that we will observe 10–11 events, which will correspond to a 95% CL limit on $\sigma_{WH} \approx$ 8 *pb*.

The procedure described for calculating the 95% CL limit on the WH production cross-section is a Bayesian calculation. There is some controversy in the HEP community regarding Bayesian and

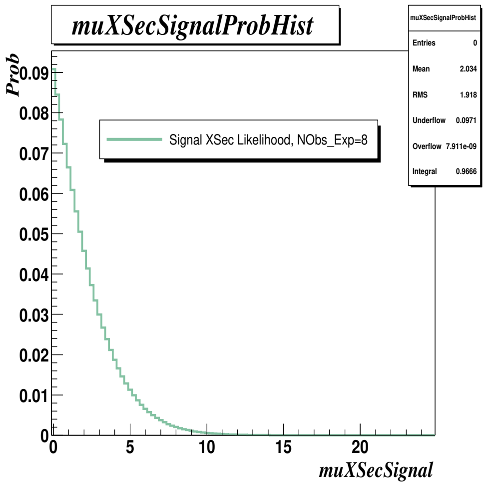

Figure 4: The σ_{WH} likelihood distribution in the scenario N_{Obs}=8 events.

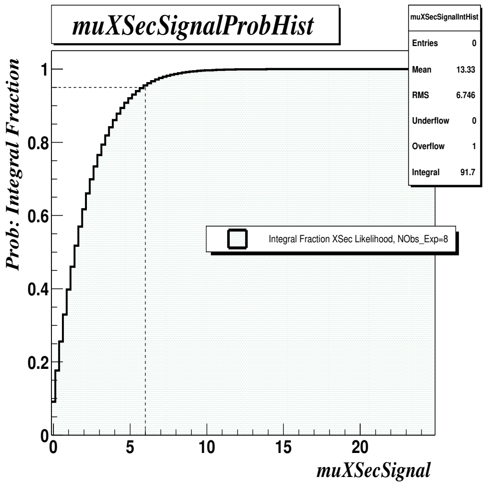

Figure 5: Fractional inverse integral plot of N_{Obs}=8 σ_{WH}likelihood distribution (Figure 4). One can see that the 95% CL limit in this N_{Obs}=8 bin is ∼6.0 *pb*.

Frequentist methods which we choose not to address here. Studies were performed using the Frequentist approach of Feldman and Cousins for the calculation of limits. The Bayesian treatment was chosen because of the consistent prescription for the incorporation of systematic errors, which is the focus of the remainder of this note. It should be noted that for some N_{Obs} values, the Feldman-Cousins method produced smaller 95% CL limits, and that this Frequentist method yielded a slightly smaller *a priori* limit (see Table 3 for a small number of N_{Obs} examples). But without a consistent technique for incorporating systematic errors, the Frequentist approach is disregarded.

N_{Obs}	σ_{WH} Limit (pb)
2	3.4
3	3.7
4	4.0
5	4.4
6	4.9
7	5.4
8	6.0
9	6.7
10	7.4
11	8.2
12	9.1
13	10.1
14	11.1
15	12.1
16	13.2
17	14.3
18	15.4
19	16.6
20	17.7
21	18.8
22	20.0

Table 2: The 95% CL limit on σ_{WH} for a few values of N_{Obs}. These limit values do not incorporate the effect of systematic errors.

6 Impact of Systematic Errors

The measurement of a limit on the WH production cross-section — or any limit, for that matter — is not as neat and tidy as the prescription described in Section 5. In the treatment above, we measured the efficiency for selecting signal and background events from samples of simulated events generated by Monte Carlo programs. These simulated collisions were then input to the CDF Run 1 detector

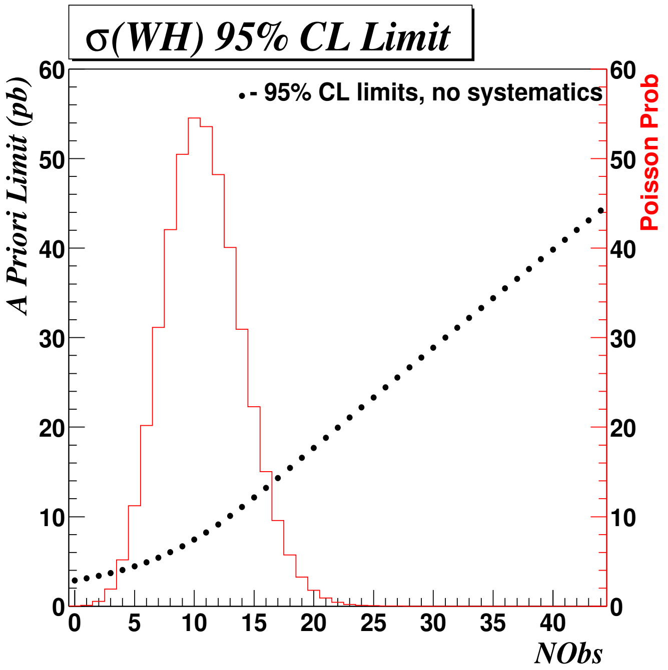

Figure 6: Poisson probability distribution with mean, variance $N_{exp}^{S,theory}$+N_{exp}^{B}=10.75 (right axis) overlayed with a graph of the 95% CL limit, both plots as a function of N_{Obs}.

simulation, and our selection criteria was applied to the measurable quantities that approximate the detector's response to the outgoing particles from these collisions. Overall efficiencies were calculated for each signal and background channel, and, along with cross section and luminosity values, expectation values for each channel were calculated.

However we know there are uncertainties on the event expectations we have calculated. We know that these Monte Carlo programs occasionally make approximations at particular points in their generation of physics collisions; what impact do these choices have on our efficiency measurements, which rely on these Monte Carlo events for input? We have a final state that includes a lepton, a neutrino (which manifests itself as $\not\!\!E_T$) and two jet objects; therefore any shortcomings of the simulation of the detector to leptons and jets and their energy measurements will correspond to mis-measured efficiencies for such final states. The Run 1 luminosity was not measured exactly (105.1 pb^{-1}); how do we incorporate a ~4% uncertainty on this value(105.1 $\pm 4pb^{-1}$)?

The answers to these questions will be pursued in the following sections. A few caveats should be noted before we embark on the in-depth discussion of the inclusion of systematic errors. First, the effect of systematics will only be studied with regard to signal and the two largest background sources: $t\bar{t}$ and W+QCD(Class 3), which constitute ~85% of the predicted background sample passing

N_{Obs}	σ_{WH} Limit (pb) Bayesian	Frequentist
5	4.4	2.5
10	7.4	6.9
15	12.1	13.2
20	17.7	18.9
A priori limit (pb)	8.4	8.1

Table 3: A comparison of Bayesian and Frequentist 95% CL limits for a few N_{Obs} scenarios.

all selection criteria. Systematics for all W+QCD(Class 3) backgrounds will be approximated by $W+b\,\bar{b}$ production only; because of the shape similarities between each of the Class 3 backgrounds(see [2]) this approximation is not without reason. The effect of systematic errors in background Classes 4 and 5 (Class 4: single top; Class 5: diboson, $Z+X$) will not be measured directly. Instead we will use the average of the cumulative systematic uncertainties on the expected number of $t\bar{t}$ and $W+b\,\bar{b}$ events to define the uncertainty on the expectations from Classes 4 and 5. This is a reasonable approximation since the Class 4 and Class 5 backgrounds account for only 15% of the total expected sample after advanced selection.

6.1 Jet Energy Scale

There are several uncertainties in the correction factors that are applied to jet energies. The basis of these jet corrections include:

- relative energy scale – correcting for any η dependence in the jet energy measurement
- absolute energy scale – corrections from attempts to determine incoming particles' energies from calorimeter response in testbeam and actual Run 1 data
- extraneous event activity – more than one p-$\overline{p}$ interaction within the same event will affect how well jet energies are measured
- energy spillage from considerably wide jets – we define a jet to lie within a cone of radius 0.4; this correction takes into account jet energy beyond this cone.

The effect of these energy scale uncertainties was measured by adjusting each of the contributing parameters by ± 1 σ, remaking our ntuples and then re-measuring the efficiencies for WH, $t\bar{t}$, and W+b $\bar{b}$. The portion of the event selection that is most affected by this systematic effect is the 2-jet requirement. Figure 7 shows the distribution of the number of E_T>20 GeV, | η |<2.0 jets for each sample being considered here (we call this number $N_{Jets}^{HighET,cent}$). We see in Figure 7(b), for example, that the $t\bar{t}$ efficiency for this requirement decreases ~8% when the energy scale uncertainties are shifted $+1\sigma$, and the $t\bar{t}$ jet-selection efficiency increases by ~8% when the energy scale uncertainties are shifted -1σ. This is a consequence of the nature of the $N_{Jets}^{HighET,cent}$ distribution for $t\bar{t}$, which is peaked in the 3 and 4 jet bin. As the jet energy scale is decreased by 1σ, some fraction of $\geq$3 jet events are demoted to the 2 jet bin when the energies of one or more of their jets are shifted below our E_T>15 GeV threshold. Similarly, when the jet energy scale is increased by 1σ, 1 jet events with other, weaker jet objects that nominally fail our jet selection, are promoted to the 2 jet bin. The converse of this argument is evident through the effect in the W+b $\bar{b}$ sample, whose $N_{Jets}^{HighET,cent}$ distribution peaks in the 0 and 1 jet bin. The $N_{Jets}^{HighET,cent}$ distribution for WH peaks in the 2 jet bin, so one would expect to see as much promotion and demotion for both of the $\pm\sigma$ scenarios, essentially washing out the effect, which we do see some evidence for.

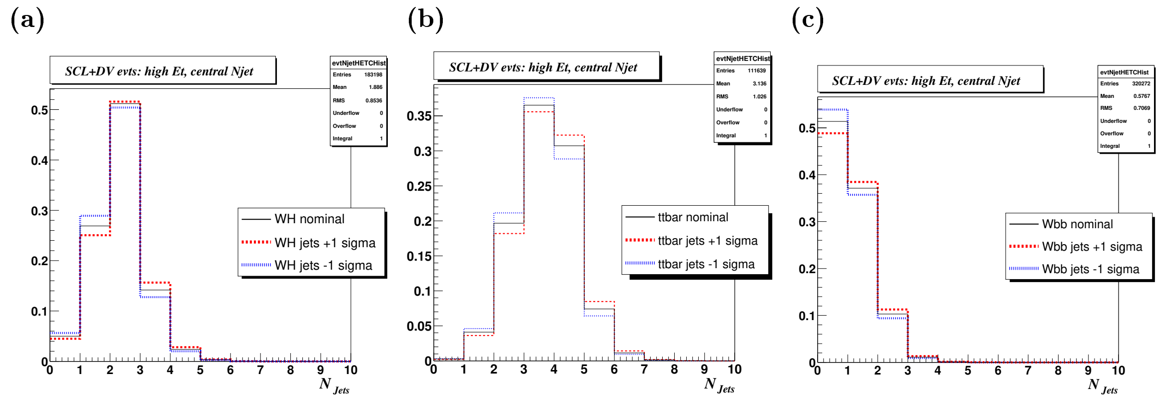

Figure 7: Effect of varying the jet energy scale uncertainties ± 1 σ on WH, $t\bar{t}$, and W+b $\bar{b}$ samples on the number of E_T>20 GeV, | η |<2.0 jets.

While we have focused on the effect of this systematic on the jet selection, it should be noted that the jet energy scale systematic effect also affects other portions of the event selection, most prominently the dijet mass requirement, $80 GeV$<$M_{j_1 j_2}$<150 GeV. The change in jet energies can also affect the neural

	Efficiency Change (%)		
	WH	$t\bar{t}$	$W{+}b\,\bar{b}$
Shift Correction Factors -1σ	-2.7	13.7	-6.1
Shift Correction Factors +1σ	0.6	-11.3	6.6

Table 4: Efficiency changes in % when shifting the factors contributing to the jet energy corrections by $\pm 1\ \sigma$.

network selection, but this effect is expected to small since we were careful not to rely too heavily on jet-E_T influenced variables as our inputs. Although the details are not reported here, the effect in these requirements was studied and was shown to be significantly smaller($\sim$3%) than in the jet selection($\sim$8%).

Later in this note we will discuss our implementation of pseudoexperiments in the construction of smeared likelihood distributions. Care was taken to preserve the correlations among the efficiency changes in Table 4 between each channel. This was accomplished by approximating the uncertainties in the jet energy correction factors with a Gaussian with mean zero and unit variance, selecting the shift in correction factor randomly from this Gaussian in each pseudoexperiment, and then mapping out the response in the efficiency change according to a linear fit to the values in Table 4. Such a method ensures that the unphysical scenario in which signal and both background channels fluctuated up or down simultaneously is avoided. Figure 8 shows the selection efficiencies for WH, $t\bar{t}$, and $W{+}b\,\bar{b}$ over 10000 pseudoexperiments.

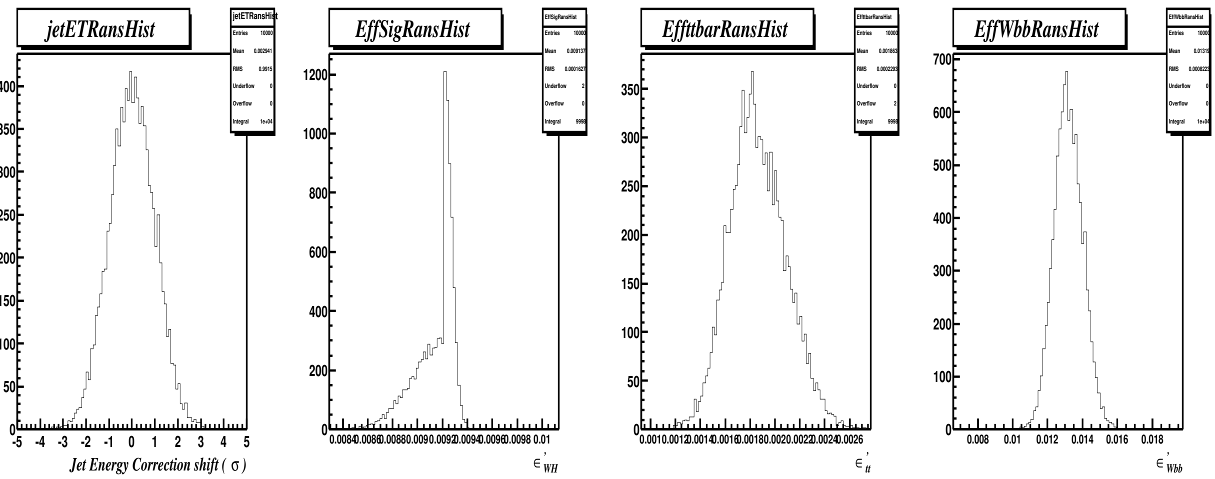

Figure 8: Distribution of efficiency changes in pseudoexperiments due to jet energy scale effects. Correlations between WH, $t\bar{t}$and $W{+}b\,\bar{b}$ channels are preserved.

6.2 Radiation Modeling

Monte Carlo generators do a fine job providing experimenters with simulated collisions showered to final states with which to understand detector response and the impact of selection criteria. However, there are underlying models in these programs that have some inherent uncertainty. For example, the modeling of initial state radiation(ISR) — radiated gluons off p- or $\overline{p}$-constituent partons — is not completely understood, and in order to achieve reasonable results with these programs some assumptions were made.

The amount of initial state radiation can affect the number of jets in each event. This is a sensitive issue, considering that we have a somewhat strict N_{Jets}=2 requirement. To evaluate the impact that ISR has on our selection efficiency, we generate WH, $t\bar{t}$, and W+$b\,\bar{b}$ samples using Pythia for the parton shower and request all ISR be OFF[1], and then re-measure the cumulative efficiency changes.

We quantify the effect of ISR as half the absolute difference between the nominal efficiency and the no-ISR efficiency:

$$\delta\epsilon^{ISR} \equiv \frac{|\epsilon^{noISR} - \epsilon^{0}|}{2\epsilon^{0}} \tag{4}$$

With this prescription we measure the effect of over-estimating the amount of ISR in our samples by looking at the extreme case in which all ISR is removed. It is clear that considering such a scenario in which there is no ISR is unphysical. Thus we approximate the impact of ISR as half the difference between the nominal and no-ISR scenarios. We also assume that an underestimate of the ISR in our samples will have an equivalent efficiency change as measured with the no-ISR samples.

Similarly, there are some uncertainties encountered in the models of final state radiation (FSR). To evaluate the impact of FSR, one does not have the luxury of simply turning off FSR in Pythia[2]. Instead one must look at the subset of no-ISR events that have all their jets matched to partons from the hard scatter; such events are assumed to have had no hard gluon emissions and can then be considered to be essentially a no-ISR+no-FSR sample. We then define quantify the effect of FSR with respect to the

[1] This is done using switch mstp(61): 1=on, 0=off.

[2] This is not true, actually. One can turn off FSR in Pythia, but this also turns off the soft gluon emissions that give jets their shapes, which is a quality that we absolutely must retain.

no-ISR sample:

$$\delta\epsilon^{FSR} \equiv \frac{|\epsilon^{noISR,noFSR} - \epsilon^{noISR}|}{2\epsilon^{noISR}} \tag{5}$$

Figure 9 shows the N_{Jets} distribution for the nominal and no-ISR samples. The N_{Jets} plots for the no-ISR+no-FSR samples were not included because our matching criteria biases these samples, yielding N_{Jets} shapes that are not easily reconciled with the FSR efficiency effects. In Figure 9 we see that initial state radiation has a $\sim$10% effect on the WH and $t\bar{t}$ 2-jet selection efficiency. The effect of ISR in the W+$b\ \bar{b}$ sample is much smaller; it is not clear why this is, but there may be some influence due to W+$b\ \bar{b}$ production itself being an initial state radiation type of event. Perhaps when we turn OFF ISR, we are only really turning off second order radiations in these types of events. This remains to be understood. For each channel, the effects of ISR in the other selection criteria (like the tagging and $M_{j_1 j_2}$ requirements) were small.

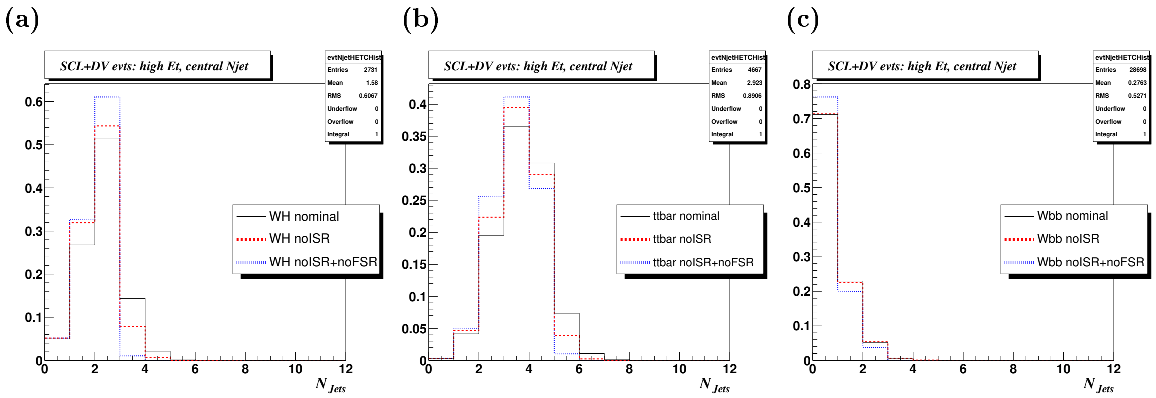

Figure 9: Effect of absence of initial state and initial state+final state radiation on WH, $t\bar{t}$, and W+$b\ \bar{b}$ samples on the number of E_T>20 GeV, | η |<2.0 jets.

The effect of FSR is smaller in WH than ISR ($\sim$5%). However FSR plays a more significant role in the backgrounds, where the effect imparts a 10% uncertainty on the $t\bar{t}$ efficiency and a 15% uncertainty on the W+$b\ \bar{b}$. These effects are again mostly due to changes in the jet selection efficiency; the effect in the neural network cut and $M_{j_1 j_2}$ requirement is small.

6.3 Parton Distribution Functions

When generating p-$\overline{p}$ collisions, some model of the structure of the proton must be employed. There is some uncertainty associated with these parton distribution functions(PDFs), and these uncertainties could have an effect on our signal and background efficiencies.

Pythia v6.129a [3]was used to generate the WH and $t\bar{t}$ samples. The default PDF choice in that version of Pythia was GRV94L [4], a leading order calculation. The W+$b\ \bar{b}$ samples were generated with ALPGEN [5]; unfortunately, ALPGEN does not have GRV94L as part of its linked PDF library. So the W+$b\ \bar{b}$ samples was generated with CTEQ5L [6], another leading order calculation from the CTEQ group.

To gauge the effect of these PDF choices, new Pythia samples were generated using CTEQ5L instead of GRV94L, and new ALPGEN W+$b\ \bar{b}$ samples were generated using MRST01 [7]. The efficiencies for WH,$t\bar{t}$, and W+$b\ \bar{b}$ were re-evaluated using these new samples. The effect on the selection efficiency was defined:

$$\delta\epsilon^{PDF} \equiv \frac{|\epsilon^{newPDF} - \epsilon^{0}|}{\epsilon^{0}} \tag{6}$$

The PDF choice changed the WH and $t\bar{t}$ efficiencies by only a few percent. The effect in W+$b\ \bar{b}$ was slightly larger, $\delta\epsilon^{PDF}_{Wb\bar{b}} = 8\%$. These values are not significantly different from other, similar Run 1 $\ell\nu b\bar{b}$ final state analyses[3].

6.4 Signal and Background Generators

Besides the PDF choice, there could be other sources of systematic error arising from the choice of Monte Carlo generator used for constructing our signal and background samples. Some possible scenarios where such issues could become important:

- the calculation could be neglecting a subset of Feynman diagrams for the desired process
- approximations could be made that are wrong or inappropriate

[3]Much larger $\delta\epsilon^{PDF}$ values were reported at the 4/30 Higgs meeting; these values were the result of bugs in the efficiency determination and have been resolved.

- mistakes could have been made in the calculations

We must guard against systematic error arising from the generator used to construct our samples. The effect of such generator-induced systematic errors is evaluated with new signal and background samples, this time generated with a different Monte Carlo program. To estimate the systematic error due to using Pythia for the WH and $t\bar{t}$ samples, we generate WH and $t\bar{t}$ samples using ALPGEN and re-measure the selection efficiencies. To estimate the systematic error due to generating W+$b\,\bar{b}$ using ALPGEN, we use a Pythia W+$b\,\bar{b}$ sample generated for another analysis.

We define the effect on the selection efficiency this way:

$$\delta\epsilon^{Gen} \equiv \frac{|\epsilon^{newGen} - \epsilon^{0}|}{\epsilon^{0}} \tag{7}$$

It should be noted that our ALPGEN W+$b\,\bar{b}$ sample was generated with loose parton-level demands: we asked for two outgoing b-partons from the hard scatter satisfying $p_T > 0.0$, $\mid \eta \mid < 15.0$, and $\Delta R(b_1, b_2) > 0.0$. Because of the time required to generate W+$b\,\bar{b}$ events, we utilized the Pythia W+$b\,\bar{b}$ sample from the latest Run 1 single top search [8]. However in this sample we did not have the freedom to make equivalent parton-level demands as were imposed in the ALPGEN sample. Dissimilar parton-level cuts on the MC samples could yield misleading efficiency effects that are not generator induced per se. For this reason, we assume that uncertainties associated with the generator choice will have only a minor effect on the basic event selection. Other Run 1 analyses have estimated the effect due to generator choice to be ~4% for the basic selection we are utilizing in this analysis. We then consider only generator-induced effects on the advanced selection efficiencies, the neural network and $M_{j_1 j_2}$ cuts. We find that the generator choice imposes a 12-13% shift on the $t\bar{t}$ and W+$b\,\bar{b}$ selection efficiencies, while the effect is very small in WH.

6.5 The Top Quark Mass

The top quark mass was measured in Run 1 to be approximately 175 ± 5 GeV. For our Monte Carlo $t\bar{t}$ samples, we demanded however that m_t=175. We seek to quantify the effect of the ± 5 GeV uncertainty on the measured top mass on our $t\bar{t}$ selection.

To evaluate this effect, we generate with Pythia new $t\bar{t}$ samples, one sample with m_t= 170 GeV and another sample with m_t= 180 GeV. We define the effect on the $t\bar{t}$ efficiency to be the largest of these two scenarios. We find that for m_t= 170 GeV, the $t\bar{t}$ efficiency increases by 2% , but in the case m_t= 180 GeV, the $t\bar{t}$ efficiency decreases by 5.6%. We define the effect on the $t\bar{t}$ efficiency to be the largest of these two scenarios. We assume that the uncertainty on m_t has no impact on the WH and W+$b\,\bar{b}$ samples.

6.6 Other Systematic Effects

There are a few more systematic uncertainties that we must account for. Thankfully, the uncertainty in the b-tagging, the lepton identification, the Run 1 high p_T lepton trigger, and the Run 1 luminosity measurement have been studied previously, allowing us to use their results directly. Table 5 has a summary of the b-tagging systematic, which varies in each channel according to the tag efficiency (the uncertainty from tagging was determined to be 10% of its value; we also insert a 10% uncertainty on our tagging scale factor [1]). The leptonID and high p_T lepton trigger uncertainties were measured in tandem; the uncertainty on the product of these efficiencies was determined to be 10% as well. Given that ϵ_{lepID}=0.854 and ϵ_{trig}=0.903 [1] we find that these effects change the efficiency in each channel by 7.7% . Finally the uncertainty on the Run 1 luminosity measurement affects the expected number of events in each channel in the same way as any change in efficiency. Thus we must account for this 4% effect because the Run 1 luminosity was determined to be 105.1 $\pm$4 pb^{-1} [10].

	WH	$t\bar{t}$	W+$b\,\bar{b}$
Prior-to-scaling ϵ_{tag} (%)	32.5$\pm$ 3.3	37.3$\pm$ 3.7	33.9$\pm$ 3.4
Scale Factor	1.08$\pm$ 0.11	1.08$\pm$ 0.11	1.08$\pm$ 0.11
Post-scaling ϵ_{tag} (%)	35.1$\pm$ 4.9	40.4$\pm$ 5.7	37.3$\pm$ 5.2
Uncertainty (% of ϵ_{tag})	14.0	14.0	14.0

Table 5: The effect of the 14% uncertainty on ϵ_{tag} for WH, $t\bar{t}$, and W+$b\,\bar{b}$.

6.7 Summary

We have investigated several sources of systematic error in this analysis, a search for $WH \rightarrow \ell\nu b\bar{b}$ in the Run 1 data. We attempted to be sensitive to effects that affected measurement of the efficiency for identifying an $\ell\nu b\bar{b}$ final state. Table 6 contains a summary of all the systematic effects considered in this analysis. For the purposes of calculating the cumulative effects, the larger of the $\pm 1\ \sigma$ uncertainties for the jet energy scale was used. We see that we will know the expected number of signal WH events to 21% ; we do a bit worse in the backgrond channels, only being able to determine the expectations to within ~30% . We use these numbers for the signal and backgrounds to approximate the systematic effect in Classes 4 and 5 as possessing a 25% uncertainty as well.

Table 7 lists a summary of the expected number of events in each Class including these systematic effects(Table 7 is just an updated version of Table 1 from Section 4). These results are consistent with other Run 1 analyses in the lepton+jets channel [9], [10].

	Efficiency Change (%)		
Effect	WH	$t\bar{t}$	$W{+}b\ \bar{b}$
jet energy corrections -1σ	-2.7	13.7	-5.9
jet energy corrections +1σ	0.6	-11.3	6.7
ISR	10.4	10.9	1.7
FSR	5.7	10.8	14.9
PDF	3.8	3.2	8.3
Generator	0.2	12.1	13.1
m_t	0.0	5.6	0.0
LepID+Trigger	7.7	7.7	7.7
Tagging	14.0	14.0	14.0
Luminosity	3.8	3.8	3.8
Cumulative	20.7	29.7	27.9

Table 6: A summary of the systematic effects influencing this analysis for signal WH and the two largest backgrounds, $t\bar{t}$ and $W{+}b\ \bar{b}$.

	Class 1	Class 2	Class 3	Class 4	Class 5
Type of Events	WH	$t\bar{t}$	W+$b\ \bar{b}$,W+$c\ \bar{c}$,W+c , W+mistags, non-W	Single top (W-*gluon* and $W*$)	WZ,WW,ZZ, Z+$b\ \bar{b}$, Z+$c\ \bar{c}$, $Z \to \tau\tau$
Luminosity	105.1	105.1	105.1	105.1	105.1
Cross Section(pb)	0.14	6.5		1.7, 0.73	
Basic Efficiency	1.2E-2	8.0E-3			
Basic N_{exp}	0.19	5.4	22.7	2.5	2.7
Advanced Efficiency	0.781	0.249	0.319	0.355	0.439
Final N_{exp}	0.15 ± 0.03	1.3 ± 0.4	7.2 ± 2.0	0.9 ± 0.2	1.2 ± 0.3

Table 7: Run 1 event expectations with systematic uncertainties on signal and backgrounds.

7 Limit Calculation Including Systematic Effects

The spirit of the calculation does not change very much from what was described in Section 5. However, where previously we used a single-valued efficiency for WH, $t\bar{t}$, and W+$b\ \bar{b}$ events, now one must replace these efficiencies with functions that incorporate the uncertainty that is evident from the studies outlined above. This technique is called *smearing* the likelihood and is a somewhat standard practice when dealing with the effects of systematic error.

We must perform integrals similar to those in Equation 2 but now there are a few more terms in the integrands. Equation 2 is replaced by:

$$0.95 = \frac{\int_{\sigma_{WH}=0}^{\sigma_{WH}^{95}} \int_{\epsilon=0}^{\infty} d\epsilon d\sigma_{WH} \mathcal{L}(Lum, \epsilon_{WH}, \epsilon_{t\bar{t}}, \epsilon_{Wbb}, \sigma_{WH} | N_{Obs}) * \mathcal{G}(\epsilon_{WH}, \delta\epsilon_{WH}) * \mathcal{G}(\epsilon_{t\bar{t}}, \delta\epsilon_{t\bar{t}}) * \mathcal{G}(\epsilon_{Wbb}, \delta\epsilon_{Wbb})}{\int_{\sigma_{WH}=0}^{\infty} \int_{\epsilon=0}^{\infty} d\epsilon d\sigma_{WH} \mathcal{L}(Lum, \epsilon_{WH}, \epsilon_{t\bar{t}}, \epsilon_{Wbb}, \sigma_{WH} | N_{Obs}) * \mathcal{G}(\epsilon_{WH}, \delta\epsilon_{WH}) * \mathcal{G}(\epsilon_{t\bar{t}}, \delta\epsilon_{t\bar{t}}) * \mathcal{G}(\epsilon_{Wbb}, \delta\epsilon_{Wbb})} \quad (8)$$

In the above expression, ϵ_i represents the nominal efficiency for channel i, and $\delta\epsilon_i$ represents the uncertainty for each channel reported in Table 6. This expression will be evaluated for each value of N_{Obs} as before.

It is potentially quite a chore to integrate these expressions by hand. Instead we perform a large number of *pseudoexperiments* in order to construct the smeared likelihoods properly, which can then be integrated numerically, saving us time. In our pseudoexperiments we perform the following procedure a large number of times for each N_{Obs} scenario:

1. Gaussian fluctuate the efficiency for each channel according to each systematic effect.

2. This yields new WH, $t\bar{t}$, and $W{+}b\,\bar{b}$ efficiencies ($\epsilon'_{WH}, \epsilon'_{t\bar{t}}, \epsilon'_{Wbb}$), and a new luminosity($Lum'$).

3. Construct the pseudoexperiment likelihood, $\mathcal{L}_{pse}(Lum', \epsilon'_{WH}, \epsilon'_{t\bar{t}}, \epsilon'_{Wbb}, \sigma_{WH}|N_{Obs})$

4. Add $\mathcal{L}_{pse}$ to an ensemble likelihood $\mathcal{L}^{\star}$

We note again that in these pseudoexperiments, the correlations in the WH, $t\bar{t}$, and $W{+}b\,\bar{b}$ samples induced by fluctuating the parameters that contribute to the jet energy scale uncertainty (one of the dominant systematics) are preserved. (See Figure 8.) The Gaussians we use to fluctuate the efficiency in each pseudoexperiment have means equal to the efficiency before fluctuation and variance equal to $\delta\epsilon$ for each effect. After a large number of pseudoexperiments the normalized version of $\mathcal{L}^{\star}$ is the smeared likelihood we seek. This distribution can then be integrated numerically to determine the 95% CL limit in the N_{Obs} bin in question:

$$0.95 = \frac{\int_0^{\sigma^{95}_{WH}} d\sigma_{WH}\mathcal{L}^{\star}(\sigma_{WH}|N_{Obs})}{\int_0^{\infty} d\sigma_{WH}\mathcal{L}^{\star}(\sigma_{WH}|N_{Obs})} \tag{9}$$

Figure 10(a)-(f) contains the $\mathcal{L}^{\star}$ distribution for a variety of N_{Obs} values. We see that in fact these smeared likelihoods have means and widths deviated from the nominal cases.We then follow this procedure to calculate the 95% CL limit in each of the N_{Obs} bins. Table 8 contains the limit values for a number of N_{Obs} scenarios, represented graphically in Figure 11 overlayed with the baseline Poisson. We see that the limit on WH in the most likely outcomes of the Run 1 is $\sim$8 pb. We can then use Equation 3 to calculate the *a priori* limit including systematic effects. We find:

$$\sigma^{95,apriori}_{WH} = 10.0pb \qquad \text{(with systematics) for } M_H\text{= } 120\ GeV$$

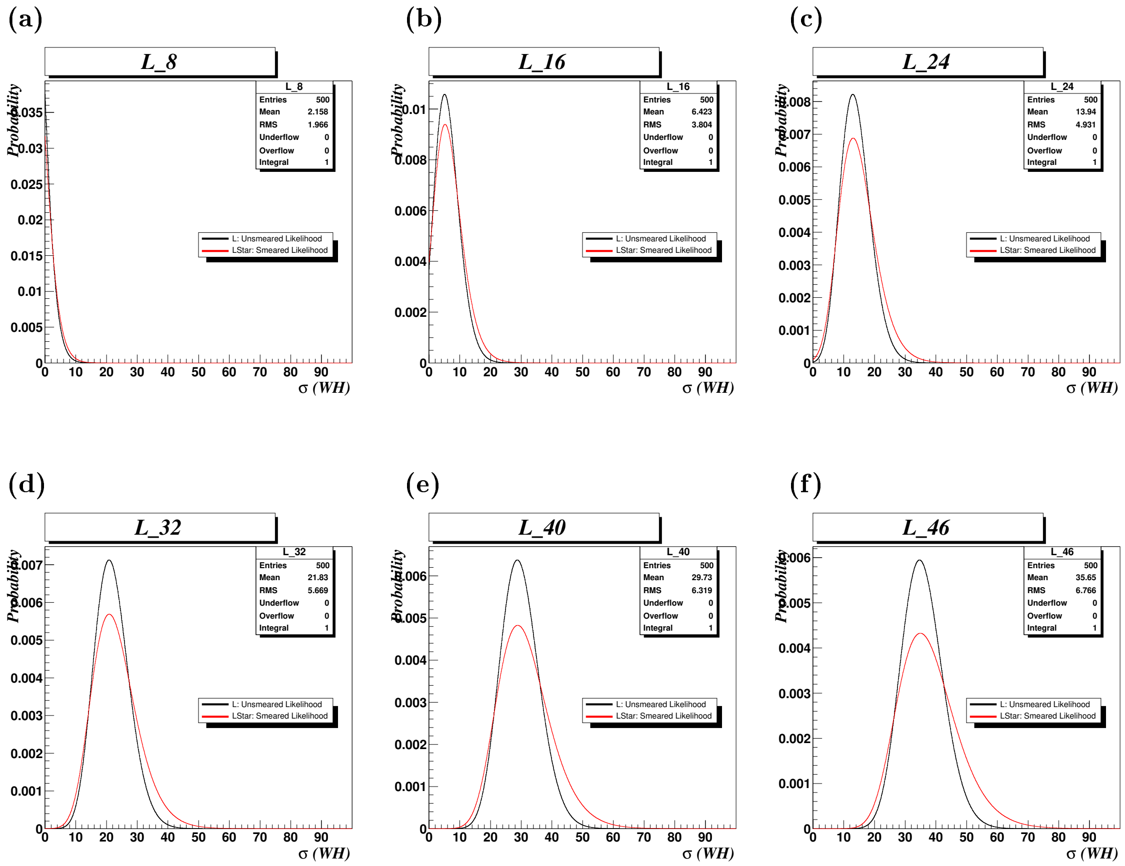

Figure 10: A comparison of unsmeared and smeared σ_{WH} likelihoods for a few N_{Obs} values.

8 Extension to Other M_H Values

The description in this document has up to now considered only the M_H=120 GeV hypothesis. The extension of the analysis to other M_H is values is straightforward. It has been shown[4] that the NN trained with the $M_H=$ 120 signal sample is adequate for other M_H values as well. This is reasonable to expect since by construction we avoided input variables that were sensitive to the di-jet mass $M_{j_1 j_2}$.

The di-jet mass requirement did however have to be re-optimized for other M_H values. Recall that in our description of the M_H=120 analysis, as our final advanced selection requirement we demanded $80 < M_{j_1 j_2} < 150\ GeV$. Clearly this $M_{j_1 j_2}$ requirement is not a good choice for $M_H > 140$ as our requirement will cut out a large amount of signal while letting unnecessary background levels at low $M_{j_1 j_2}$. This cut

[4]See pre-blessing talk of 5/15/03. A study was performed that compared the *a priori* limit for the hypothesis M_H=140 GeV using the network trained with the $M_H=$ 120 sample and a network trained with a M_H=140 sample. There was basically no impact on the limit.

N_{Obs}	σ_{WH} Limit (pb)
2	3.9
3	4.3
4	4.8
5	5.3
6	5.8
7	6.5
8	7.2
9	8.0
10	8.9
11	9.8
12	10.8
13	11.9
14	13.1
15	14.2
16	15.3
17	16.6
18	17.8
19	19.2
20	20.4
21	21.8
22	23.1

Table 8: The 95% CL limit on σ_{WH} for a few values of N_{Obs} including the effect of systematic errors.

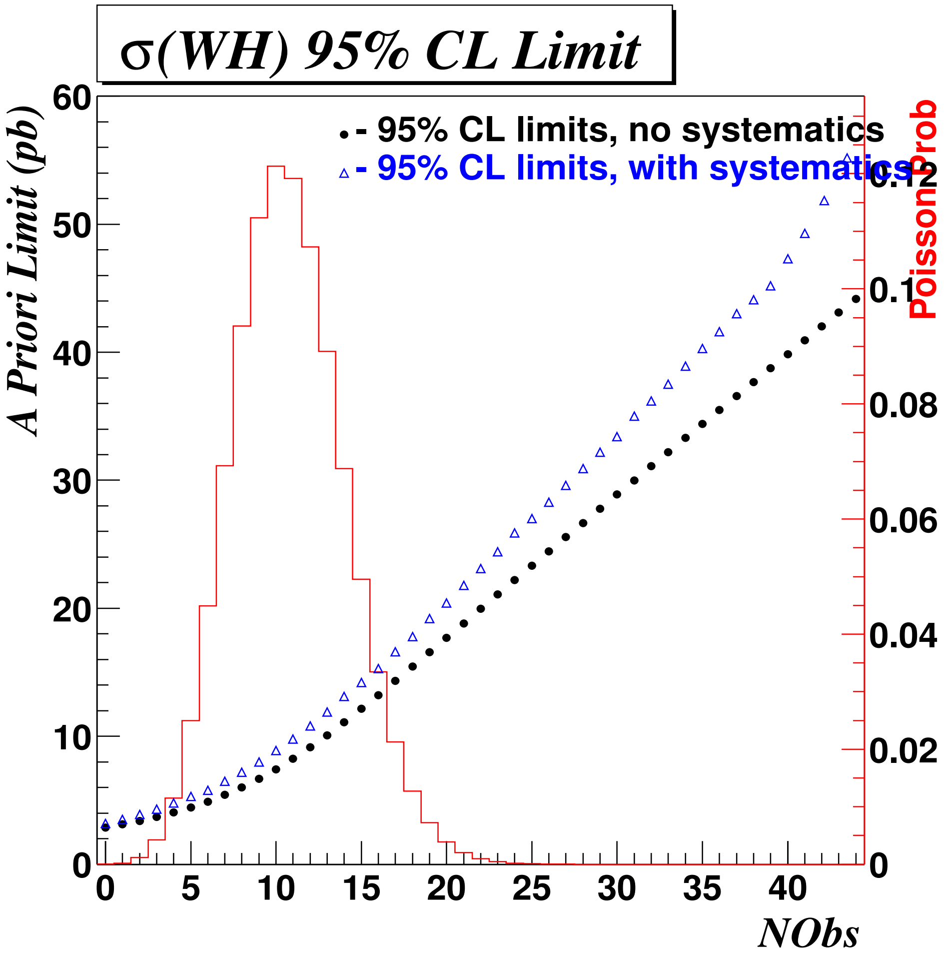

Figure 11: Poisson probability distribution with mean, variance $N_{exp}^{S,theory}+N_{exp}^{B}$=10.53 (right axis) overlayed with a graph of the 95% CL limit(left axis), both plots as a function of N_{Obs}, including impact of systematic errors.

was re-optimized for each M_H value, and the final $M_{j_1 j_2}$ requirement for each M_H hypothesis is listed in Table 9.

With the final portion of the selection defined in Table 9 we essentially have a slightly different analysis for each M_H value. The numbers of expected events passing all selection for signal and background are listed in Appendix A. The effect of systematic errors was addressed in the same way described in Section 6 for M_H=110 and 140. The systematic effects for M_H= 100,130, and 150 were approximated via fit from the three M_H values for which the effects were measured. Appendix A contains other figures relevant to these studies at other M_H values: the fits for the systematic effects are illustrated in Figure 12, and Table 11 contains a summary of the systematic effects as a function of M_H .

M_H	$M_{j_1 j_2}$ Window
100	$60 < M_{j_1 j_2} < 130$
110	$70 < M_{j_1 j_2} < 140$
120	$80 < M_{j_1 j_2} < 150$
130	$90 < M_{j_1 j_2} < 160$
140	$100 < M_{j_1 j_2} < 170$
150	$110 < M_{j_1 j_2} < 180$

Table 9: Optimized $M_{j_1 j_2}$ requirements for each M_H value considered in this analysis.

	A priori Limit (pb)	
M_H	No Systematics	With Systematics
100	9.5	11.3
110	8.4	9.9
120	8.4	10.0
130	9.3	10.9
140	13.5	15.6
150	24.3	28.5

Table 10: *A priori* limit as a function of M_H before and after the inclusion of systematic effects.

Table 10 contains a comparison of the *a priori* limit as a function of M_H both before and after the inclusion of systematic effects. We see that the *a priori* limit is in the range 10-11 pb for $M_H < 130$ GeV ; however the limit increases significantly for $M_H > 130$ GeV. This is due to the small branching ratio of $H \to b\bar{b}$ for larger M_H values. As M_H grows the number of $\ell\nu b\bar{b}$ final state WH events decreases; thus our signal expectation gets smaller and smaller, making it more and more difficult to establish a limit at the same level as in the scenarios $M_H < 130$.

9 Summary

In this note we have described the Bayesian technique that has been employed in the calculation of the 95% CL limit on σ_{WH} as a function of the possible outcomes of our Run 1 experiment. The calculation has been described both before and after the inclusion of the effects of systematic errors. The different systematic effects were also described in detail. Our event expectations agree with previous Run 1 analyses. Our final *a priori* limit on the WH production cross section for the mass hypothesis M_H= 120 GeV is 10.0 pb. The incorporation of systematic effects increases this limit by 19% over the equivalent calculation neglecting systematics.

We have completed an extension of this analysis to other M_H values and determined the *a priori* limit for a variety of low M_H values. The *a priori* limit is in the range 10-11 pb for $M_H < 130$ GeV and the limit is somewhat larger for larger M_H values.

References

[1] CDF 6304, "Acceptance Calculation for $WH \to \ell\nu b\bar{b}$ Search"

[2] CDF 6309, "Neural Network Implementation for a $WH \to \ell\nu b\bar{b}$ Search"

[3] T. Sjostrand, Computer Physics Commun. 82 (1994) 74.

[4] M. Gluck, E. Reya and A. Vogt, Z. Phys. C **67**, 433 (1995).

[5] M. L. Mangano, M. Moretti, F. Piccinini, R. Pittau and A. D. Polosa, arXiv:hep-ph/0206293.

[6] H. L. Lai *et al.*, Phys. Rev. D **51**, 4763 (1995) [arXiv:hep-ph/9410404].

[7] Need citation for this PDF

[8] C. Ciobanu, "Using A Neural Network to Identify Single Top in Run 1 Data", CDF 5742

[9] CDF 4112, "Search for New Particles $X \to b\bar{b}$ Produced in Association with W ..."

[10] T. Affolder *et al.* [CDF Collaboration], Phys. Rev. D **64**, 032002 (2001) [arXiv:hep-ex/0101036].

[11] CDF 6468, "Results from a New Run 1 $WH \to \ell\nu b\bar{b}$ Search"

Appendix

A Summary of Systematic Effects for other M_H Values

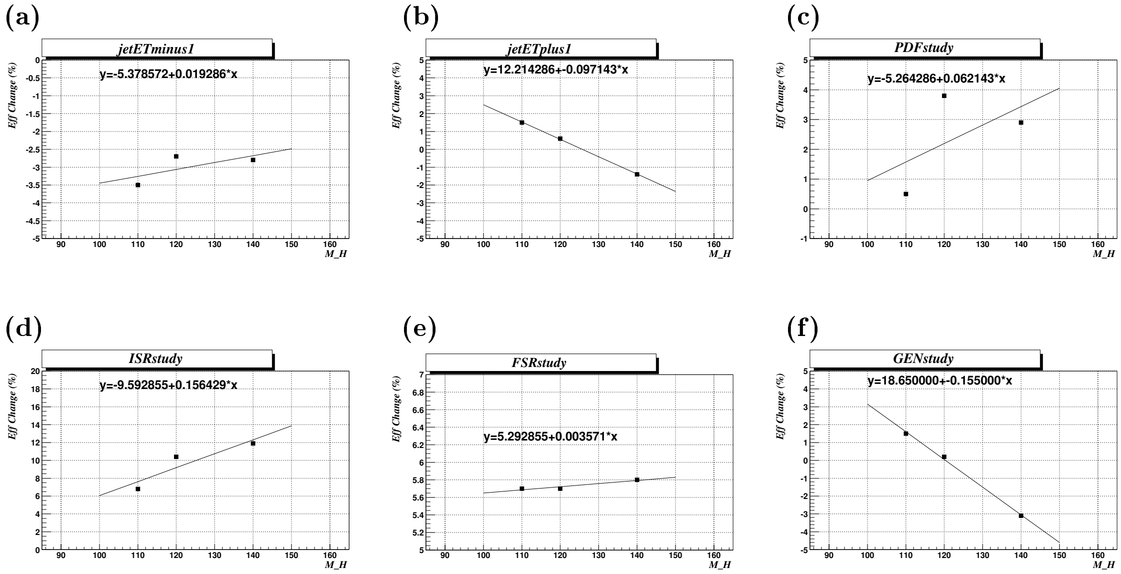

Figure 12: Effect of absence of initial state and initial state+final state radiation on WH, $t\bar{t}$, and $W{+}b\ \bar{b}$ samples on the number of $E_T{>}20\ GeV$, $\mid \eta \mid{<}2.0$ jets.

Effect	WH Efficiency Change (%) M_H=100 GeV	M_H=110	M_H=120	M_H=130	M_H=140	M_H=150
jet energy corrections -1σ	-3.5	-3.5	-2.7	-2.9	-2.8	-2.5
jet energy corrections +1σ	2.5	1.5	0.6	-0.4	-1.4	-2.4
ISR	6.1	6.8	10.4	10.7	11.9	13.9
FSR	5.7	5.7	5.7	5.8	5.8	5.8
PDF	1.0	0.5	3.8	2.8	2.9	4.1
Generator	3.2	1.5	0.2	1.5	3.1	4.6
m_t	0.0	0.0	0.0	0.0	0.0	0.0
LepID+Trigger	7.7	7.7	7.7	7.7	7.7	7.7
Tagging	14.0	14.0	14.0	14.0	14.0	14.0
Luminosity	3.8	3.8	3.8	3.8	3.8	3.8
Cumulative	19.1	19.1	20.7	20.9	21.7	23.3

Table 11: A summary of the systematic effects influencing this analysis for signal WH at a variety of M_H values. The impact of the systematic effects were measured directly in the M_H=110,120, and 140 GeV samples; the effects were then fit to get the impact for M_H=100,130,150.

	Class 1	Class 2	Class 3	Class 4	Class 5
Type of Events	WH M_H= 100	$t\bar{t}$	W+$b\,\bar{b}$,W+$c\,\bar{c}$,W+c , W+mistags, non-W	Single top (W-*gluon* and $W*$)	WZ,WW,ZZ, Z+$b\,\bar{b}$, Z+$c\,\bar{c}$, $Z \to \tau\tau$
Luminosity	105.1	105.1	105.1	105.1	105.1
Cross Section(pb)	0.26	6.5		1.7, 0.73	
Basic Efficiency	1.10E-2	8.00E-3			
Basic N_{exp}	0.32	5.4	22.7	2.5	2.7
Advanced Efficiency	0.796	0.260	0.386	0.349	0.567
Final N_{exp}	0.25 ± 0.05	1.4 ± 0.4	8.8 ± 2.5	0.9 ± 0.2	1.5 ± 0.4

Table 12: Run 1 event expectations with systematic uncertainties on signal WH and its backgrounds for hypothesis M_H= 100 GeV.

	Class 1	Class 2	Class 3	Class 4	Class 5
Type of Events	WH M_H= 110	$t\bar{t}$	W+$b\,\bar{b}$,W+$c\,\bar{c}$,W+c , W+mistags, non-W	Single top (W-*gluon* and $W*$)	WZ,WW,ZZ, Z+$b\,\bar{b}$, Z+$c\,\bar{c}$, $Z \to \tau\tau$
Luminosity	105.1	105.1	105.1	105.1	105.1
Cross Section(pb)	0.18	6.5		1.7, 0.73	
Basic Efficiency	1.20E-2	8.00E-3			
Basic N_{exp}	0.24	5.4	22.7	2.5	2.7
Advanced Efficiency	0.813	0.268	0.367	0.364	0.529
Final N_{exp}	0.20 ± 0.04	1.4 ± 0.4	8.3 ± 2.3	0.9 ± 0.2	1.4 ± 0.4

Table 13: Run 1 event expectations with systematic uncertainties on signal WH and its backgrounds for hypothesis M_H= 110 GeV.

	Class 1	Class 2	Class 3	Class 4	Class 5
Type of Events	WH M_H= 130	$t\bar{t}$	W+$b\ \bar{b}$,W+$c\ \bar{c}$,W+c , W+mistags, non-W	Single top (W-*gluon* and $W*$)	WZ,WW,ZZ, Z+$b\ \bar{b}$, Z+$c\ \bar{c}$, $Z \rightarrow \tau\tau$
Luminosity	105.1	105.1	105.1	105.1	105.1
Cross Section(pb)	0.10	6.5		1.7, 0.73	
Basic Efficiency	1.10E-2	8.00E-3			
Basic N_{exp}	0.12	5.4	22.7	2.5	2.7
Advanced Efficiency	0.730	0.233	0.267	0.340	0.339
Final N_{exp}	0.09 ± 0.02	1.3 ± 0.4	6.1 ± 1.7	0.9 ± 0.2	0.9 ± 0.2

Table 14: Run 1 event expectations with systematic uncertainties on signal WH and its backgrounds for hypothesis M_H= 130 GeV.

	Class 1	Class 2	Class 3	Class 4	Class 5
Type of Events	WH M_H= 140	$t\bar{t}$	W+$b\ \bar{b}$,W+$c\ \bar{c}$,W+c , W+mistags, non-W	Single top (W-*gluon* and $W*$)	WZ,WW,ZZ, Z+$b\ \bar{b}$, Z+$c\ \bar{c}$, $Z \rightarrow \tau\tau$
Luminosity	105.1	105.1	105.1	105.1	105.1
Cross Section(pb)	0.08	6.5		1.7, 0.73	
Basic Efficiency	8.0E-3	8.00E-3			
Basic N_{exp}	0.07	5.4	22.7	2.5	2.7
Advanced Efficiency	0.654	0.215	0.203	0.303	0.220
Final N_{exp}	0.04 ± 0.01	1.2 ± 0.4	4.6 ± 1.3	0.8 ± 0.2	0.6 ± 0.2

Table 15: Run 1 event expectations with systematic uncertainties on signal WH and its backgrounds for hypothesis M_H= 140 GeV.

	Class 1	Class 2	Class 3	Class 4	Class 5
Type of Events	WH M_H= 150	$t\bar{t}$	W+$b\ \bar{b}$,W+$c\ \bar{c}$,W+c , W+mistags, non-W	Single top (W-*gluon* and $W*$)	WZ,WW,ZZ, Z+$b\ \bar{b}$, Z+$c\ \bar{c}$, $Z \rightarrow \tau\tau$
Luminosity	105.1	105.1	105.1	105.1	105.1
Cross Section(pb)	0.06	6.5		1.7, 0.73	
Basic Efficiency	5.0E-3	8.00E-3			
Basic N_{exp}	0.03	5.4	22.7	2.5	2.7
Advanced Efficiency	0.526	0.182	0.173	0.263	0.147
Final N_{exp}	0.02 ± 0.005	1.0 ± 0.3	3.9 ± 1.1	0.7 ± 0.2	0.4 ± 0.1

Table 16: Run 1 event expectations with systematic uncertainties on signal WH and its backgrounds for hypothesis M_H= 150 GeV.

	σ_{WH} Limit (pb)					
N_{Obs}	M_H=100 GeV	110	120	130	140	150
0	3.3	3.0	3.2	3.8	6.0	11.7
1	3.6	3.2	3.5	4.2	6.8	13.5
2	3.9	3.6	3.9	4.7	7.7	15.5
3	4.3	3.9	4.3	5.2	8.8	18.0
4	4.7	4.3	4.8	5.8	10.0	20.8
5	5.2	4.7	5.3	6.5	11.4	24.0
6	5.7	5.2	5.8	7.3	13.0	27.7
7	6.3	5.7	6.5	8.2	14.7	31.5
8	6.9	6.3	7.2	9.2	16.6	35.8
9	7.6	7.0	8.0	10.3	18.8	40.5
10	8.4	7.7	8.9	11.5	21.0	45.3
11	9.2	8.4	9.8	12.7	23.4	50.4
12	10.1	9.2	10.8	14.1	25.8	55.2
13	11.0	10.1	11.9	15.4	28.2	60.2
14	12.1	11.1	13.1	16.9	30.9	65.1
15	13.2	12.1	14.2	18.4	33.3	70.1
16	14.3	13.1	15.3	19.8	35.6	74.4
17	15.4	14.2	16.6	21.4	38.4	78.4
18	16.6	15.2	17.8	22.9	40.9	81.9
19	17.8	16.3	19.2	24.5	43.4	85.1
20	19.0	17.5	20.4	26.0	46.1	87.5
21	20.4	18.7	21.8	27.6	48.6	90.0
22	21.7	19.9	23.1	29.2	51.3	91.9
23	22.9	21.0	24.4	30.7	53.7	93.2
24	24.2	22.1	25.9	32.5	56.7	94.3
25	25.4	23.2	27.0	33.9	58.9	95.2
26	27.0	24.6	28.3	35.4	61.3	96.0
27	28.1	25.7	29.6	37.0	63.9	96.5
28	29.5	26.9	30.9	38.5	66.3	97.0
29	30.9	28.1	32.2	40.0	68.8	97.4
30	32.1	29.2	33.4	41.4	70.9	97.7
31	33.5	30.5	35.0	43.3	73.9	98.0
32	34.8	31.6	36.2	44.8	75.9	98.2
33	36.1	32.8	37.5	46.4	78.2	98.4
34	37.4	34.0	38.9	48.0	80.5	98.5
35	38.8	35.2	40.3	49.6	82.5	
36	40.0	36.3	41.6	51.1	84.3	
37	41.3	37.5	43.0	52.8	86.2	
38	42.8	38.8	44.1	54.2		
39	44.1	39.9	45.2	55.5		
40	45.3	41.1	47.3	58.0		
41	46.8	42.5	48.1	58.8		
42	48.0	43.5	49.4	60.4		
43	49.2	44.6	50.7			
44	50.8	46.0	52.2			
45	51.9	47.0	53.3			
46	53.4	48.4	54.5			

Table 17: The 95% CL limit on σ_{WH} for values of N_{Obs} including the effect of systematic errors.